CONF-970201--32

Influence of Neutron Energy Spectrum on Primary Damage Formation*

Roger E. Stoller[1] and Lawrence R. Greenwood [2]

[1] Metals and Ceramics Division
Oak Ridge National Laboratory
Oak Ridge, TN 37831-6376 USA

[2] Materials and Chemistry Division
Pacific Northwest National Laboratory
Richland, WA 99352 USA

presented at 1997 TMS Symposium on Materials for Spallation Neutron Sources, to be submitted for publication to TMS

*Research sponsored by the Office of Nuclear Regulatory Research, U.S. Nuclear Regulatory Commission under inter-agency agreement DOE 1886-8109-8L with the U.S. Department of Energy and by the Division of Materials Sciences, U.S. Department of Energy under contract DE-AC05-96OR22464 with Lockheed Martin Energy Research Corp., and the Office of Fusion Energy, U.S. Department of Energy at the Pacific Northwest National Laboratory.

DISCLAIMER

Influence of Neutron Energy Spectrum on Primary Damage Formation

Roger E. Stoller[1] and Lawrence R. Greenwood [2]

[1] Metals and Ceramics Division
Oak Ridge National Laboratory
Oak Ridge, TN 37831-6376 USA

[2] Materials and Chemistry Division
Pacific Northwest National Laboratory
Richland, WA 99352 USA

Abstract

Displacement cascade formation in iron has been investigated by the method of molecular dynamics (MD) for cascade energies up to 40 keV. The results of these simulations have been used to obtain effective, energy-dependent cross sections for two measures of primary damage production: (1) the number of surviving point defects expressed as a fraction of the those predicted by the standard secondary displacement model by Norgett, Robinson, and Torrens (NRT), and (2) the fraction of the surviving interstitials contained in clusters that formed during the cascade event. The primary knockon atom spectra for iron obtained from the SPECTER code have been used to weight these MD-based damage production cross sections in order to obtain spectrally-averaged values for several locations in commercial fission reactors, materials test reactors, a DT fusion reactor first wall, and a pulsed spallation neutron source. An evaluation of these results indicates that neutron energy spectrum differences between the various environments do not lead to significant differences between the average primary damage formation parameters. This conclusion implies that the displacement damage component of radiation damage produced in a high energy spallation neutron source should be well simulated by irradiation in a fission reactor neutron spectrum, and that differences in nuclear transmutation production may be a greater source of uncertainty in the prediction of material performance in the planned National Spallation Neutron Source.

*Research sponsored by the Office of Nuclear Regulatory Research, U.S. Nuclear Regulatory Commission under inter-agency agreement DOE 1886-8109-8L with the U.S. Department of Energy and by the Division of Materials Sciences, U.S. Department of Energy under contract DE-AC05-96OR22464 with Lockheed Martin Energy Research Corp., and the Office of Fusion Energy, U.S. Department of Energy at the Pacific Northwest National Laboratory.

Introduction

Although charged-particle irradiation experiments and data from the current generation of spallation neutron sources will be helpful [1], estimates of the radiation damage expected in modern spallation sources or deuterium-tritium (DT) fusion reactors must be made largely on the basis of data obtained in fission reactors. A primary uncertainty in such use of the fission reactor data base is the potential impact of the much higher energy neutrons that are produced in both of the other irradiation environments. For example, a typical fission reactor spectrum has few neutrons above 2 to 5 MeV, while a DT fusion neutron spectrum has a peak at 14.1 MeV and neutrons can be produced at energies as high as the incident proton energy in a spallation source. In the case of the planned National Spallation Neutron Source (NSNS), this upper limit on the neutron energy is 1000 MeV [1-2]. These neutrons will in turn lead to the production of displacement damage by higher energy primary knockon atoms (PKA). In addition, the primary proton beam will produce a large fraction of the total atomic displacements, particularly in the front of the spallation target. Finally, the production rates of transmutation products (notably hydrogen and helium) from both the neutrons and the proton beam will be much higher in the NSNS environment than in a fission reactor [1-2].

The issue of PKA energy effects can be addressed through the use of displacement cascade simulations using the method of molecular dynamics (MD). Although MD simulations can provide a detailed picture of the formation and evolution of displacement cascades, they impose a substantial computational burden. However, recent advances in computing equipment permit the simulation of high energy displacement events involving more than one-million atoms [3-5]; the results presented below will encompass MD cascade simulation energies from near the displacement threshold to as high as 40 keV. Two parameters have been extracted from the MD simulations: the number of point defects that remain after the displacement event is completed and the fraction of the surviving interstitials that are contained in clusters. For the purpose of comparison with standard dosimetry, these values have been normalized to the number of atomic displacements calculated with the secondary displacement model by Norgett, Robinson, and Torrens (NRT) [6].

The energy dependence of the two MD defect parameters was used to evaluate the effects of neutron energy spectrum. Simple, energy-dependent

functional fits to the MD results were obtained, and the SPECOMP codes [7] was used to compute effective cross sections for point defect survival and point defect clustering. PKA spectra for iron obtained from SPECTER [8] were then used to weight these effective cross sections in order to calculate spectrum-averaged values for various neutron irradiation environments, including several locations in both water and sodium-moderated fission reactors, a DT fusion reactor first wall [9], and a 450 MeV spallation neutron source [10,11].

MD Cascade Simulations

The molecular dynamics code, MOLDY, and the interatomic potential for iron that was used are described in detail in Refs. 12-14. Additional details on the results obtained by this method can be found in Refs. 3-5 and 15. Briefly described, the process of conducting a cascade simulation requires two steps. First, a block of atoms of the desired size is thermally equilibrated. This process permits the lattice thermal vibrations (phonon waves) to be established for the simulated temperature, and typically requires a run of approximately 10 ps. This atom block can be saved and used as the starting point for several subsequent cascade simulations. Then, the cascade simulations are initiated by giving one of the atoms a defined amount of kinetic energy, E_{MD}, in a specified direction. This atom is equivalent to the PKA following a collision with a neutron. Statistical variability can be introduced by either further equilibration of the starting block or by choosing either a different primary knockon atom or PKA direction. Typically, at least six different cascades are required to obtain results that can be used to represent the average behavior at any one energy and temperature.

The MOLDY code describes only elastic collisions between atoms; it does not account for energy loss mechanisms such as electronic excitation and ionization. Thus, the initial energy E_{MD} given to the simulated MD PKA is analogous to the damage energy (T_{dam}) in the NRT model [6]. Using the values of E_{MD} in Table 1, the corresponding E_{PKA} and the NRT defects in iron have been calculated using the procedure described in Ref. 6 with the recommended 40 eV displacement threshold [16]. These values are also listed in Table 1. Note that the difference between the MD simulation, or damage energy, and the PKA energy increases as the PKA energy increases.

It is not simple to determine whether or not the absence of electronic

energy losses has a significant influence in the MD cascade simulations. For example, electron-phonon coupling could alter the rate of cascade cooling and either promote or inhibit defect clustering. However, the results of the cascade simulations have been shown to be broadly consistent with experimental observations [15], suggesting that the overall impact may not be large. Since the primary purpose of this paper is to make a relative comparison of different irradiation environments, modest changes to the parameters derived from the MD simulations should not alter the conclusions.

The cascade simulations are continued until the phase of incascade recombination of vacancies and interstitials is complete and the atom block has returned to near thermal equilibrium. The required time varies from about 5 ps for the low-energy cascades to 15-20 ps for the 40 keV cascades. The computing time with the MOLDY code is almost linearly proportional to the number of atoms in the simulation. Higher energy events require a larger atom block as listed in Table 1. Two to three weeks of cpu time is required to complete the highest energy 40 keV cascade simulations with 1,024,000 atoms for 15 ps on a modern high-speed workstation equipped a MIPS R8000 cpu and 256 Mbytes of memory.

Two parameters are of primary interest to this work: the number of point defects that survive after incascade recombination is complete, and the fraction of the surviving interstitials that are contained in clusters rather than as isolated defects. The former is important because it is only the surviving point defects that can contribute to radiation-induced microstructural evolution. The latter is significant because these small clusters provide nuclei for the growth of larger defects which can give rise to mechanical property changes. The formation of these small clusters directly within the cascade means that the extended defects can evolve more quickly than if the clusters could only be formed by the much slower process of classical nucleation. For purposes of this work, interstitials were considered clustered if they were within the nearest-neighbor lattice distance of another interstitial. The size distribution of the interstitial clusters produced is a function of the cascade energy [15], and the interstitial clustering fraction is calculated by summing that distribution.

The surviving MD defects can be conveniently described as a fraction of the NRT displacements [6] and the number of clustered interstitials as a fraction of the surviving MD defects. The energy dependence of the

surviving defect fraction (η) and the interstitial clustering fraction (f_{icl}) from the MD simulations is shown in Figs. 1 and 2, respectively. Because the dependence of the results on the irradiation temperature was weak, all of the results obtained at 100, 600, and 900 K are shown [3-4,15]. The line drawn through the data in each figure is a nonlinear least squares fit to the data using the following functions:

$$\eta = 0.5608 \cdot E_{MD}^{-0.3029} + 3.227x10^{-3} \cdot E_{MD} \qquad (1)$$

$$f_{icl} = [0.097 \cdot ln(E_{MD} + 0.9)]^{0.3859} - 7x10^{-6} \cdot E_{MD}^{2.5} \qquad (2)$$

where E_{MD} is in keV.

In both Eqns. (1) and (2), the first term in the function dominates the energy dependence up to about 20 keV. The second term accounts for the effect of subcascade formation at the highest energies [4,5]. Mathematically, this term is responsible for the minimum in the defect survival curve and the maximum in the interstitial clustering curve at about 20 keV. This change in the energy dependence occurs because subcascade formation makes a high single energy cascade appear to be the equivalent of several lower energy cascades. Thus, the defect survival fraction is slightly higher, and the interstitial clustering fraction slightly lower at 40 keV than at 20 keV. The increase in the defect survival fraction between 20 and 40 keV is slight, but it appears to be statistically significant from the magnitude of the standard deviations that are shown as error bars in Fig.1. Since the standard deviations on the average interstitial clustering fractions are much larger, the significance of the maximum shown in Fig. 2 is less clear. No cascades with energies higher than 40 keV have been completed at this time. However, based on the degree of subcascade formation observed in the 40 keV cascade simulations, it appears unlikely that η and f_{icl} will change significantly at higher cascade energies. Therefore, the values calculated from Eqns. (1) and (2) for 40 keV were applied for all the higher energy cascades in the SPECTER calculations.

Results of Defect Production Calculations Using SPECTER

Energy-dependent defect production cross sections for surviving MD defects and clustered interstitials, and spectrum-averaged values for several

irradiation environments were generated by modifying the SPECOMP [7] and SPECTER [8] computer codes. SPECOMP normally calculates displacement cross sections for compounds using the primary knock-on atomic recoil energy distributions contained in a 100-neutron-energy by 100-recoil-energy grid for each of 40 different elements. For the present defect and clustered interstitial calculations, these new functions were used as a factor multiplying the standard displacement cross section equations as a function of the damage energy, T_{dam}. SPECOMP thus produced surviving defect and clustered interstitial cross sections on a 100 point neutron energy grid.

The SPECTER computer code contains libraries of calculated cross sections for displacements, gas production, and total energy distribution, as well as atomic recoil energy distributions for over 40 elements and various compounds. For a given neutron energy spectrum and irradiation time, the code will calculate the net radiation damage effects, as given above. In the present case, the SPECOMP calculations for the surviving defect and clustered interstitial cross sections were added to the SPECTER libraries. SPECTER runs for various neutron spectra thereby produced spectrum-averaged values for the point defect and interstitial clustering fractions.

The neutron flux distributions and iron PKA spectra obtained from SPECTER for four irradiation facilities are shown in Figures 3 and 4, respectively. The facilities illustrated are: the Radiation Effects Facility (10,11) in the Intense Pulsed Neutron Source (IPNS REF), a 450 MeV spallation neutron source at the Argonne National Laboratory; the midcore location in the Fast Flux Test Facility (FFTF) at the U.S. DOE Hanford Reservation; the midplane of the Peripheral Target Position of the High Flux Isotope Reactor at the Oak Ridge National Laboratory (HFIR PTP); and the first wall of Starfire, a DT fusion reactor conceptual design (9). Neither the REF and nor the FFTF are currently available for conducting irradiations, but the use of their neutron spectra extends the range of the comparisons discussed below. The neutron fluxes in Figure 3 have been normalized to the maximum value for each facility to aid in the comparison of their energy dependence. The PKA spectra in Figure 4 are normalized to a single neutron-PKA interaction.

The differences in the neutron energy spectra in Figure 3 arise primarily from two sources. First, differences in the neutron source term: spallation in the IPNS, fission in the FFTF and HFIR, and DT fusion in the Starfire. Secondly, differences in the neutron moderator are illustrated by

comparing the sodium moderated FFTF with the light water moderated HFIR. In spite of these differences in neutron energy, the PKA energy spectra are relatively similar. The primary distinction that can be drawn from among these four is the higher fraction of PKAs above ~0.2 MeV for the Starfire spectrum. This is a result of the DT fusion source term at 14.1 MeV.

Results and Discussion

The primary results of these calculations are summarized in Figure 5. The PKA-spectrum-averaged defect survival fraction is shown in Figure 5a, and the interstitial clustering fraction in Figure 5b. In both cases, the effective production cross section has been divided by the NRT dpa cross section. In order to provide a broader comparison, values are shown for three irradiation sites in addition to those illustrated in Figures 3 and 4. These are: the 1/4-thickness position of a typical commercial pressurized water reactor (PWR), a position located in the removable beryllium reflector of the HFIR (RB*), and the below-core position in the FFTF (BC).

Although the lowest survival fraction is obtained in the Starfire FW as a result of the 14.1 MeV source term, the defect survival fractions shown in Figure 5a are not simply determined by how hard the initial neutron energy spectrum is. For example, the survival fractions for IPNS and both FFTF sites are greater than any of the water moderated fission reactor spectra. An examination of the results shown in Figure 4 indicates that the PKA spectra are generally dominated by PKA below 100 keV. Thus, average behavior is controlled by the details of the spectra in the low to intermediate energy region. Here the differences between the fission and spallation PKA spectra are relatively modest and this is reflected in the average values shown in Figure 5a.

Similarly, the average interstitial clustering fraction shown in Figure 5b is only weakly dependent on the initial neutron energy spectrum. The average clustering fraction tracks the defect survival fraction (since only defects that survive can cluster), but the differences among the various environments are reduced because the energy dependence of interstitial clustering is opposite to that of defect survival (see Figs. 1 and 2).

The values shown in Figure 5 indicate that the nature of the neutron displacement damage formed in a spallation neutron environment should not be significantly different from that obtained in fission reactors. The average

defect survival fraction is about 0.25 to 0.35 and the interstitial clustering fraction is about 0.15 to 0.18 for all the cases shown except the DT fusion reactor first wall. This conclusion is qualified by the fact that the SPECTER calculation for IPNS included only neutrons with energies up to 20 MeV. However, the neutron flux for the IPNS shown in Figure 3 begins to reduce sharply at high energies between 1 and 10 MeV. This reduction in the flux at high energies is reflected in the PKA spectra shown in Figure 4. In addition, the MD results shown in Figures 1 and 2 indicate that defect production from the higher energy PKAs should be similar to that produced in the 10 to 40 keV range. Taken together, these two observations suggests that the error incurred by the absence of the higher energy neutrons is probably quite modest.

Summary

Although it is not yet possible to simulate the very high energy displacement cascades that will be generated in the materials used in the NSNS target region, the analysis of MD cascade simulations in iron for energies up to 40 keV provides considerable insight. The primary damage parameters derived from the MD results exhibit a strong dependence on cascade energy up to 10 keV. This dependence is diminished and slightly reversed between 20 and 40 keV. This reversal is due to the formation of well-defined subcascades in this energy region. An analysis of the MD cascades suggests that these parameters should not change significantly at higher energies, indicating that the results reported here should be relevant to high-energy neutron sources such as DT fusion and the NSNS. Notably, the spectrally-averaged defect production cross sections calculated for several fission reactor neutron spectra were quite similar to those obtained for a spallation neutron spectrum arising from a 450 MeV proton beam on a target of depleted U-238 (IPNS).

The results presented above support the view that fission reactor data can be reliably used to estimate the radiation effects expected in a machine such as the NSNS. However, this conclusion should be considered somewhat preliminary until further work is completed. As mentioned above, SPECTER does not currently compute displacement reactions from neutrons with energies greater than 20 MeV. With an incident proton beam energy of 1000 MeV, the NSNS will have a larger fraction of neutrons above this limit than does IPNS. In addition, SPECTER does not incorporate a spallation displacement model.

Since spallation reactions make a significant contribution to the total reaction rate for neutrons above 40 MeV, accounting for these reactions is more important for the NSNS than for IPNS. Spallation reactions lead to PKA of lower mass than the primary target atoms (iron) and higher defect survival fractions are generally associated with lighter PKA. Similarly, the incident proton beam will produce many of the displacements in the front of the NSNS target by spallation and scattering reactions. The PKA masses and the PKA energy spectra generated by the proton beam will be different from those obtained from the neutron reactions.

It is difficult to estimate the magnitude of the differences arising from the effects just mentioned, but previous calculations of the neutron spectrum and atomic displacements in the Los Alamos Meson Physics Facility (LAMPF) provide some guidance. The LAMPF is a spallation source driven by an 800 MeV proton beam. About 6% of the neutrons in the measured neutron spectrum were above 20 MeV, and these neutrons accounted for 26% of the total calculated neutron dpa [17,18]. If the values of the primary damage parameters shown in Figures 1 and 2 remain relatively unchanged at higher energies as expected, the spectrally-averaged defect production cross sections for the NSNS should be similar to those already calculated for the radiation environments shown in Figure 5. In this case, the largest uncertainty regarding the use of fission reactor data for the purpose of designing the NSNS would be impact of differences in transmutation production rates between the two environments.

References

1. L. K. Mansur, J. R. DiStefano, K. Farrell, E. H. Lee, and S. J. Pawel, "Materials Considerations for the National Spallation Neutron Source Target," submitted to the American Nuclear Society for presentation at the Topical Meeting on Nuclear Applications of Accelerator Technology, Albuquerque, NM, Nov. 16-20, 1997.

2. M. S. Wechsler, C. Lin, P. D. Ferguson, L. K. Mansur, and W. F. Sommer, "Calculations of Radiation Damage in Target, Container, and Window Materials for Spallation Neutron Sources," presented at the Second Int. Conf. on Accelerator-Driven Transmutation Technologies and Applications, Kalmar, Sweden, June 3-7 1996, in press.

3. R. E. Stoller, J. Nucl. Mater. 233-237 (1996) 999-1003.

4. R. E. Stoller, JOM 48 (1996) 23-27.

5. R. E. Stoller, G. R. Odette, and B. D. Wirth, "Primary Defect Formation in bcc Iron," presented at the International Workshop on Defect Production, Accumulation, and Materials Performance in Irradiation Environments, Davos, Switzerland, October 2-8, 1996, accepted for publication in J. Nucl. Mater.

6. M. J. Norgett, M. T. Robinson, and I. M. Torrens, Nucl. Eng. and Des. 33 (1975) 50-54.

7. L. R. Greenwood, "SPECOMP Calculations of Radiation Damage in Compounds," Reactor Dosimetry: Methods, Applications, and Standardization, ASTM STP 1001, H. Farrar IV and E. P. Lippincott, Eds., American Society of Testing and Materials, West Conshohocken, PA, 1989, pp. 598-602.

8. L. R. Greenwood and R. K. Smither, "SPECTER: Neutron Damage Calculations for Materials Irradiations," ANL/FPP/TM-197, Argonne National Laboratory, Argonne, IL, January 1985.

9. "STARFIRE - A Commercial Tokomak Fusion Reactor Power Plant Study," ANL/FPP-80-1, Argonne National Laboratory, Argonne, IL, September, 1980.

10. M. A. Kirk, R. C. Birtcher, T. H. Blewitt, L. R. Greenwood, R. J. Popek, and R. R. Heinrich, J. Nucl. Mater. 96 (1981) 37-50.

11. R. C. Birtcher, T. H. Blewitt, M. A. Kirk, T. L. Scott, B. S. Brown, and L. R. Greenwood, J. Nucl. Mater. 108 & 109 (1982) 3-9.

12. M. W. Finnis, "MOLDY6-A Molecular Dynamics Program for Simulation of Pure Metals," AERE R-13182, UK AEA Harwell Laboratory (1988).

13. M. W. Finnis and J. E. Sinclair, Phil. Mag. A50 (1984) 45-55 and Erratum, Phil. Mag. A53 (1986) 161.

14. A. F. Calder and D. J. Bacon, J. Nucl. Mater. 207 (1993) 25-45.

15. W. J. Phythian, R. E. Stoller, A. J. E. Foreman, A. F. Calder, and D. J. Bacon, J. Nucl. Mater. 223 (1995) 245-261.

16. ASTM E521, Standard Practice for Neutron Radiation Damage Simulation by Charged-Particle Irradiation, Annual Book of ASTM Standards, Vol. 12.02, American Society of Testing and Materials, Philadelphia.

17. D. R. Davidson, L. R. Greenwood, R. C. Reedy, and W. F. Sommer, "Measured Radiation Environment at the Clinton P. Anderson Los Alamos Meson Pgysics Facility (LAMPF) Irradiation Facility," Effects of Radiation on Materials: 12th International Symposium, ASTM STP 870, F. A. Garner and J. S. Perrin, Eds., American Society of Testing and Materials, West Conshohocken, PA, 1985, pp. 1199-1208.

18. M. S. Wechsler, D. R. Davidson, L. R. Greenwood, and W. F. Sommer, "Calculation of Displacement and Helium Production at the Clinton P. Anderson Los Alamos Meson Pgysics Facility (LAMPF) Irradiation Facility," Effects of Radiation on Materials: 12th International Symposium, ASTM STP 870, F. A. Garner and J. S. Perrin, Eds., American Society of Testing and Materials, West Conshohocken, PA, 1985, pp. 1189-1198.

Table 1. Typical MD cascade parameters and required atom block sizes

Neutron Energy (MeV)	Average PKA Energy (keV)	Corresponding E_{MD} (keV)	NRT Displacements	Atoms in Simulation
0.0034	0.116	0.1	1	3,456
0.0058	0.236	0.2	2	6,750
0.014	0.605	0.5	5	6,750
0.036	1.24	1.0	10	54,000
0.074	2.54	2.0	20	54,000
0.19	6.6	5.0	50	128,000
0.40	13.7	10.0	100	250,000
0.83	28.8	20.0	200	250,000
1.8	61.3	40.0	400	1,024,000

Figure Captions

Figure 1. Average MD point defect survival fraction as a function of cascade energy; results of MD simulations at 100, 600 and 900 K.

Figure 2. Average in-cascade interstitial clustering fraction as a function of cascade energy; results of MD simulations at 100, 600 and 900 K.

Figure 3. Energy dependence of normalized neutron flux in various irradiation environments: IPNS (450 MeV spallation), Starfire (DT fusion), HFIR (light water moderated fission), and FFTF (sodium moderated fission).

Figure 4. Normalized iron PKA spectra from various irradiation sources: IPNS (450 MeV spallation), Starfire (DT fusion), HFIR (light water moderated fission), and FFTF (sodium moderated fission).

Figure 5. Comparison of spectrally-averaged damage production cross sections (per NRT dpa) for various irradiation environments; defect survival ratio is shown in (a) and the interstitial clustering fraction is shown in (b).

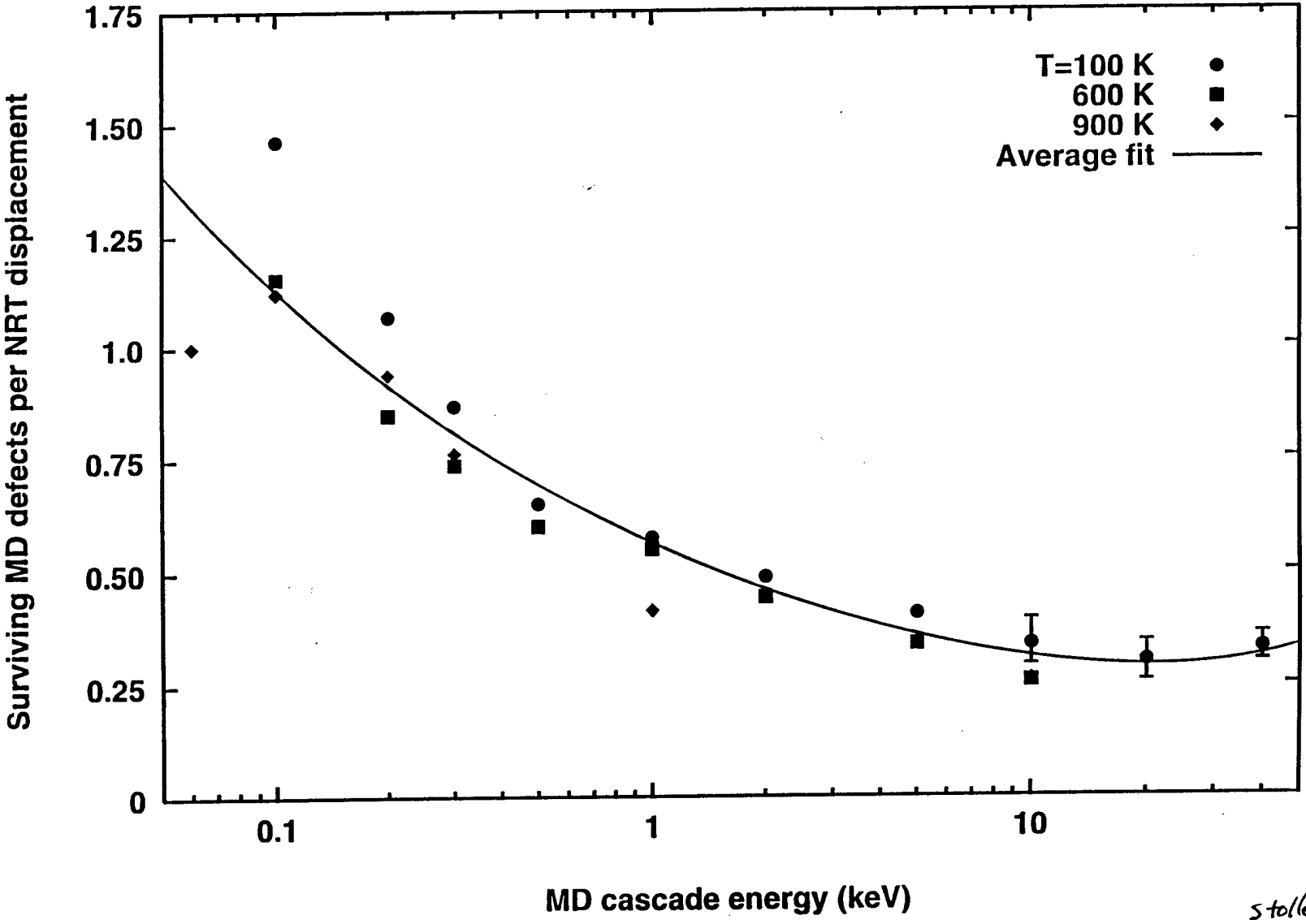

Stoller and Greenwood
Fig-1

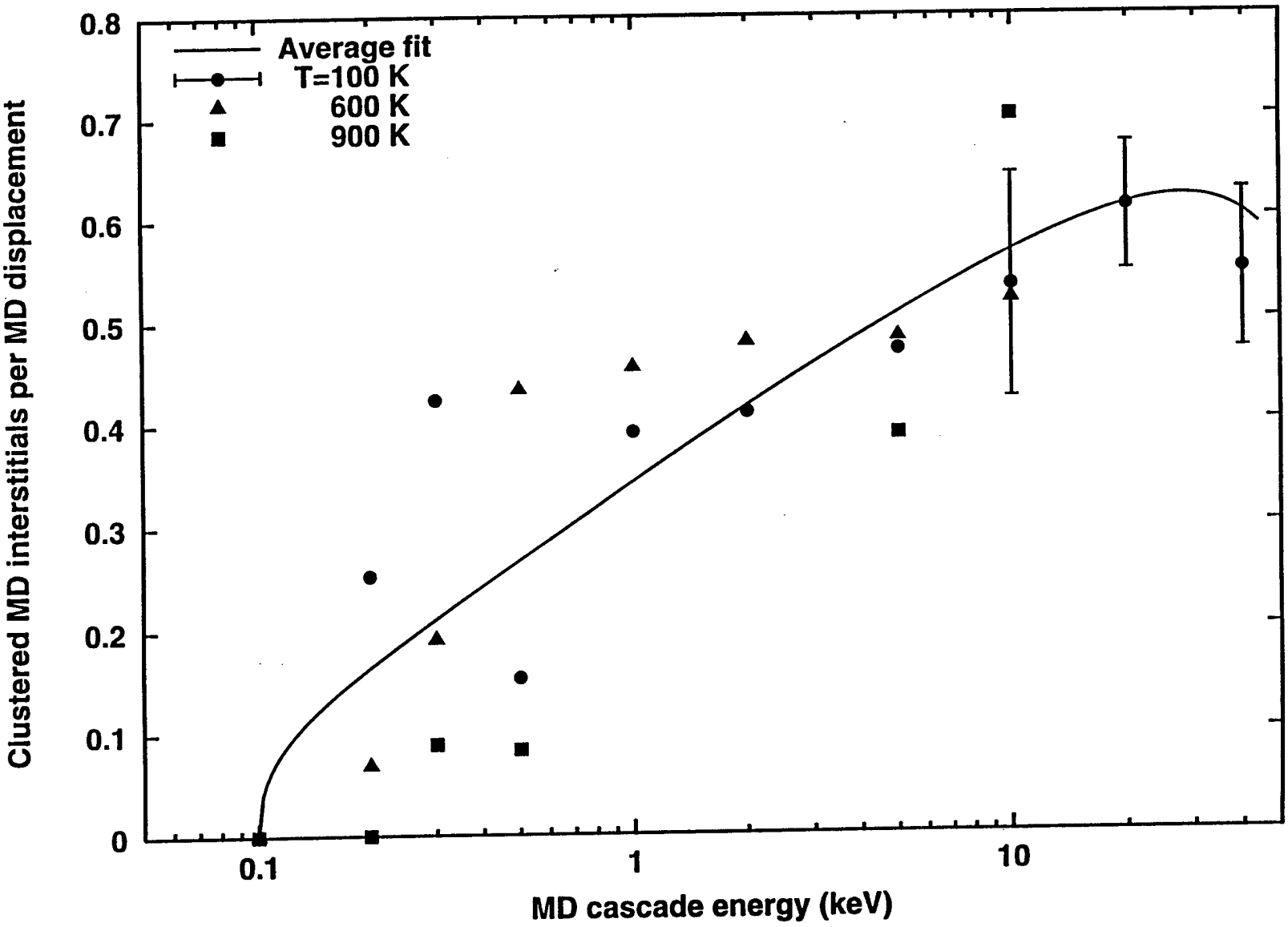

Stoller & Greenwood

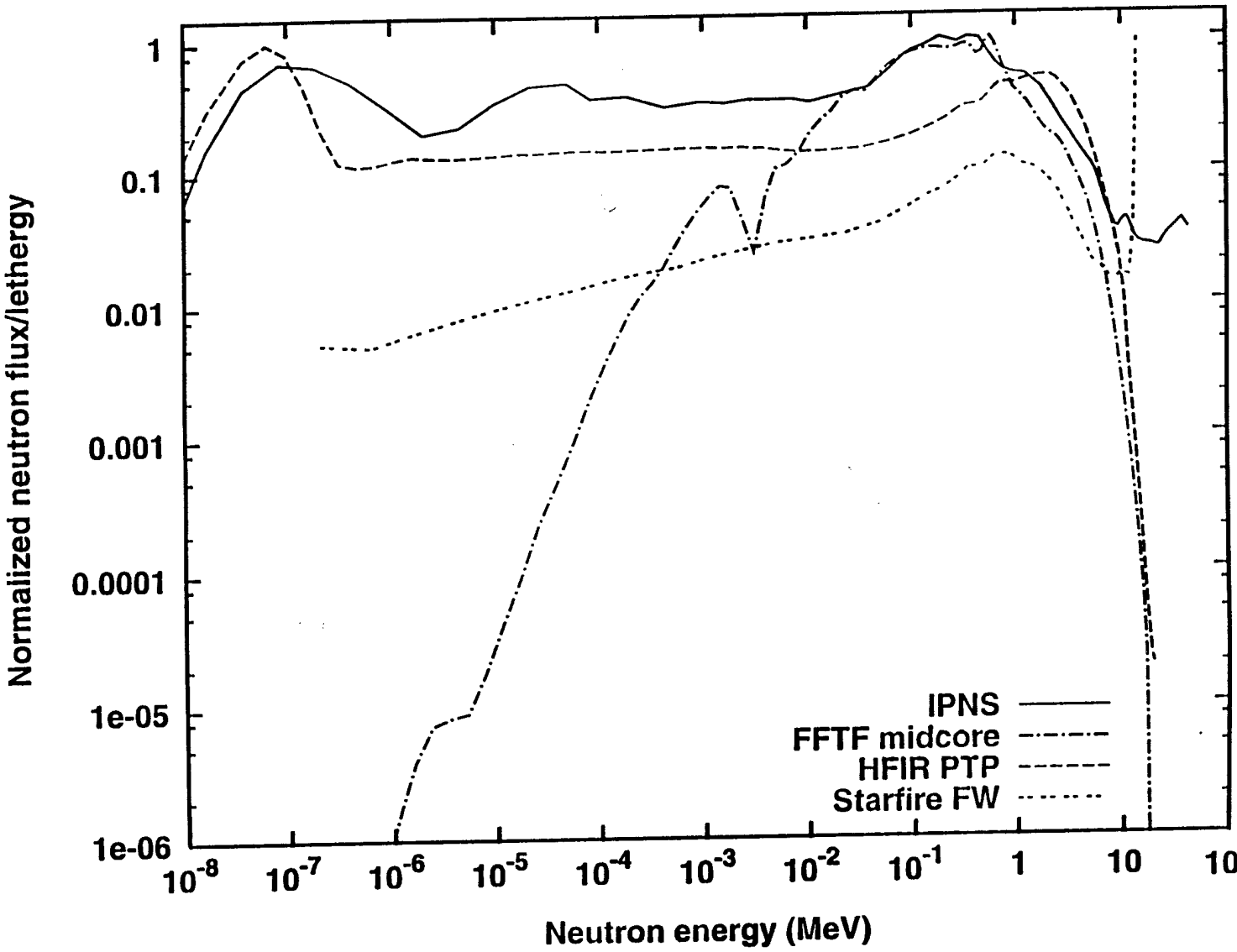

Stoller and Greenwood
Fig. 3

ORNL DWG 97-124466

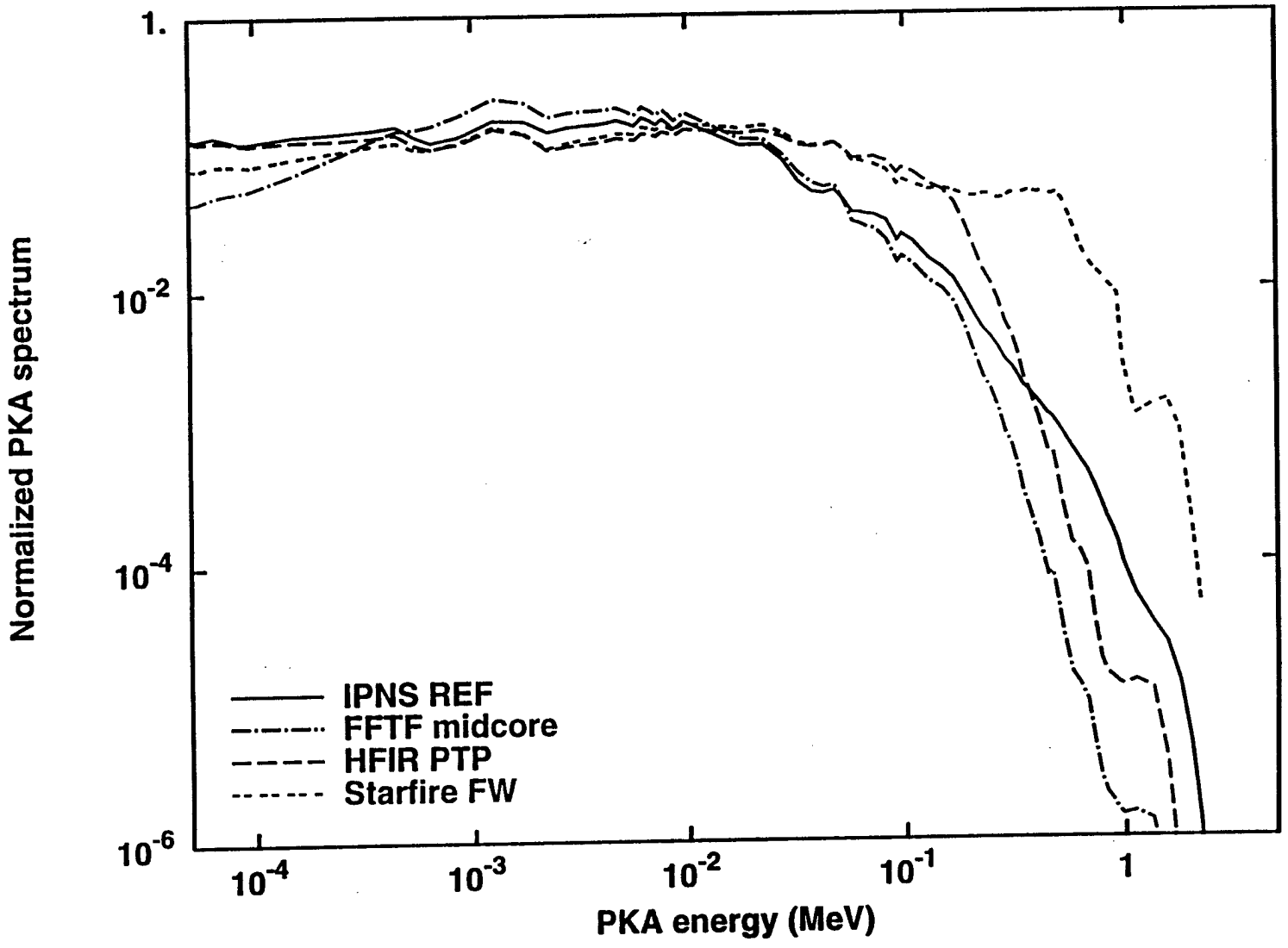

Stoller and Greenwood
Fig. 4

ORNL DWG 97-123570

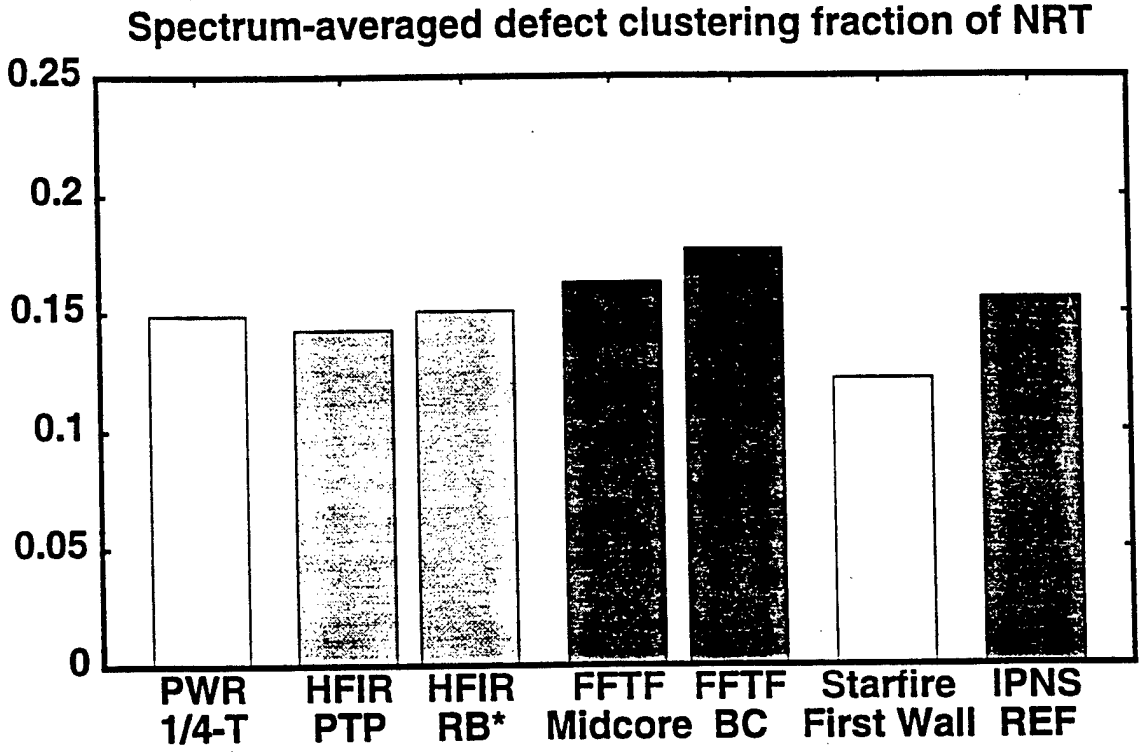

Stoller and Greenwood
Fig. 5b

ORNL DWG 97-123569

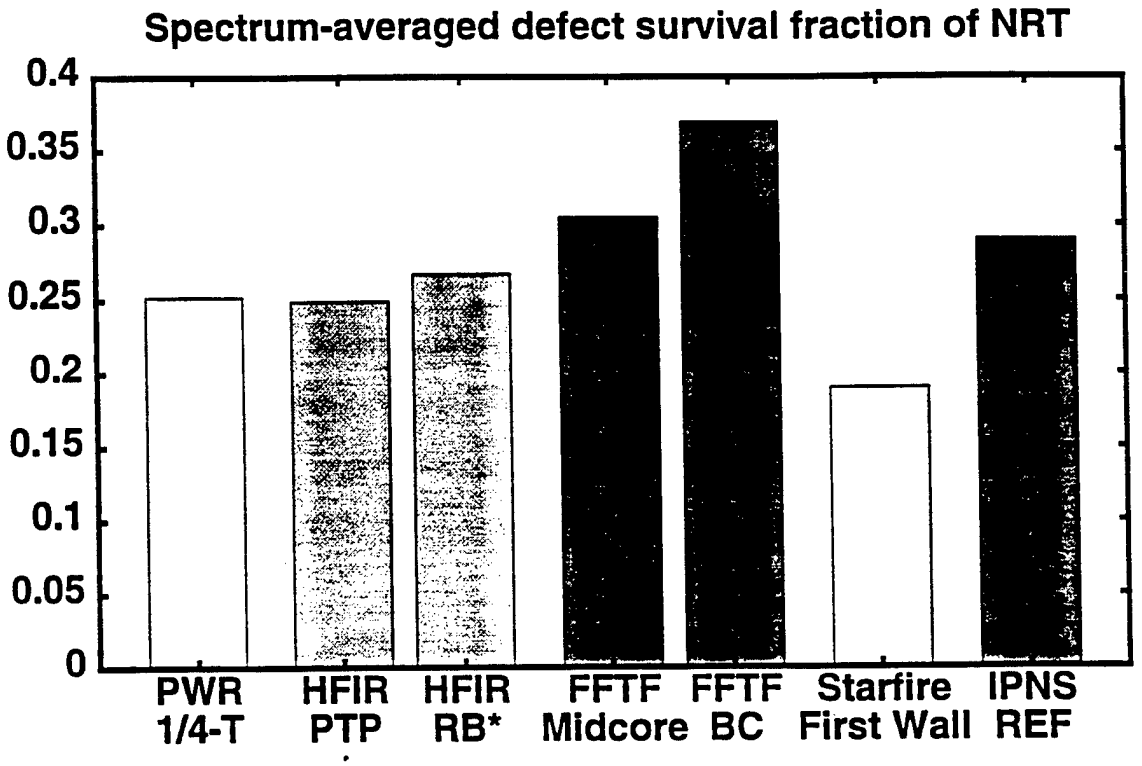

Stoller and Greenwood
Fig. 5a

DOE

(18) DOE, XF
(19) UC-900, DOE